14246

ACCURACY AND POSITION REQUIREMENTS OF REVERSE BALLISTIC EXPERIMENTS OF ROD PENETRATION INTO SIC-CERAMIC TO DETECT THE EFFECT OF FAILURE KINETICS IN CERAMICS

Th. Behner[1], C. E. Anderson Jr[2], D. L. Orphal[3], V. Hohler[1], M. Junginger[1] and D. W. Templeton[4]

[1] *Fraunhofer Institut für Kurzzeitdynamik (EMI), Eckerstr. 4, 79104 Freiburg, Germany*
[2] *Southwest Research Institute, P.O. Drawer 28510, San Antonio, TX 78228, USA*
[3] *International Research Associates, Inc., 4450 Black Avenue, Pleasanton, CA 94566, USA*
[4] *U. S. Army TACOM-TARDEC, AMSTA-TR, Warren, MI 48397 USA*

A new set of reverse ballistic experiments has been designed to overcome uncertainties in the interpretation of experimental data of two independent data sets that suggest the existence of a so–called "failure wave" for penetration into SiC-ceramics. The possible detection of such a phenomenon requires very high accuracy in experimental measurements. The accuracy and position requirements for the new experiments together with the experimental design are reported here.

INTRODUCTION

Kozhushko *et al.* [1], Orphal *et al.* [2] and Orphal and Franzen [3] combined data from two independent data sets—high-velocity penetration experiments of long-rod tungsten projectiles and shaped-charge jets into silicon carbide (SiC)—that suggest an increase in penetration resistance of SiC at impact velocities greater than about 4.5 km/s. This result was interpreted as possible evidence of a failure wave in SiC, based on plane shock experiments by Kanel *et al.* [4] and by Brar *et al.* [5] who report the detection of a failure wave in K19 glass and soda lime glass. Experiments, done by Bless *et al.* [6], report direct observation of a failure wave in Pyrex glass rods impacted by steel plates at velocities of about 200 m/s.

The experiments of [3] involved penetration of SiC by long tungsten rods at impact velocities in the range 1.5 to 4.6 km/s. Reverse ballistic testing was done. The SiC targets were launched by a two stage light gas gun. The SiC samples (density $\rho_T = 3.22$ g/cm^3) were cylindrical in shape and confined laterally by a Ti sleeve and at the front and at the rear by an Al disk. The rods were made of pure tungsten (density $\rho_P = 19.2$ g/cm^3). To prevent an influence of the lateral target dimensions, the ceramic diameter was 23.6 mm and the rod diameter was D = 0.762 mm with L/D = 15 and 20, i. e. the ratio of SiC diameter to rod diameter was 31. The penetration process was observed by applying the flash x-ray technique. The second type of experiments [1] involved the penetration of SiC by copper shaped charge jets at impact velocities from 5 to 7 km/s. Here, shorting gages were used to provide time-of-arrival data of the jet. The penetration velocities of both test series are plotted in Fig. 1 as a function of the impact velocity.

Report Documentation Page

Form Approved
OMB No. 0704-0188

1. REPORT DATE	2. REPORT TYPE	3. DATES COVERED
01 SEP 2004	**Journal Article**	**12-03-2004 to 23-08-2004**

4. TITLE AND SUBTITLE
ACCURACY AND POSITION REQUIREMENTS OF REVERSE BALLISTIC EXPERIMENTS OF ROD PENETRATION INTO SIC-CERAMIC TO DETECT THE EFFECT OF FAILURE KINETICS IN CERAMICS

5a. CONTRACT NUMBER

5b. GRANT NUMBER

5c. PROGRAM ELEMENT NUMBER

6. AUTHOR(S)
Th Behner; C Anderson; D Orphal; V Hohler; D Templeton

5d. PROJECT NUMBER

5e. TASK NUMBER

5f. WORK UNIT NUMBER

7. PERFORMING ORGANIZATION NAME(S) AND ADDRESS(ES)
International Research Associates, Inc.,,4450 Black Avenue,Pleasanton,CA,94566

8. PERFORMING ORGANIZATION REPORT NUMBER
; #14246

9. SPONSORING/MONITORING AGENCY NAME(S) AND ADDRESS(ES)
U.S. Army TARDEC, 6501 East Eleven Mile Rd, Warren, Mi, 48397-5000

10. SPONSOR/MONITOR'S ACRONYM(S)
TARDEC

11. SPONSOR/MONITOR'S REPORT NUMBER(S)
#14246

12. DISTRIBUTION/AVAILABILITY STATEMENT
Approved for public release; distribution unlimited

13. SUPPLEMENTARY NOTES

14. ABSTRACT
A new set of reverse ballistic experiments has been designed to overcome uncertainties in the interpretation of experimental data of two independent data sets that suggest the existence of a so--called "failure wave" for penetration into SiC-ceramics. The possible detection of such a phenomenon requires very high accuracy in experimental measurements. The accuracy and position requirements for the new experiments together with the experimental design are reported here.

15. SUBJECT TERMS

16. SECURITY CLASSIFICATION OF:			17. LIMITATION OF ABSTRACT	18. NUMBER OF PAGES	19a. NAME OF RESPONSIBLE PERSON
a. REPORT	b. ABSTRACT	c. THIS PAGE			
unclassified	**unclassified**	**unclassified**	**Public Release**	**13**	

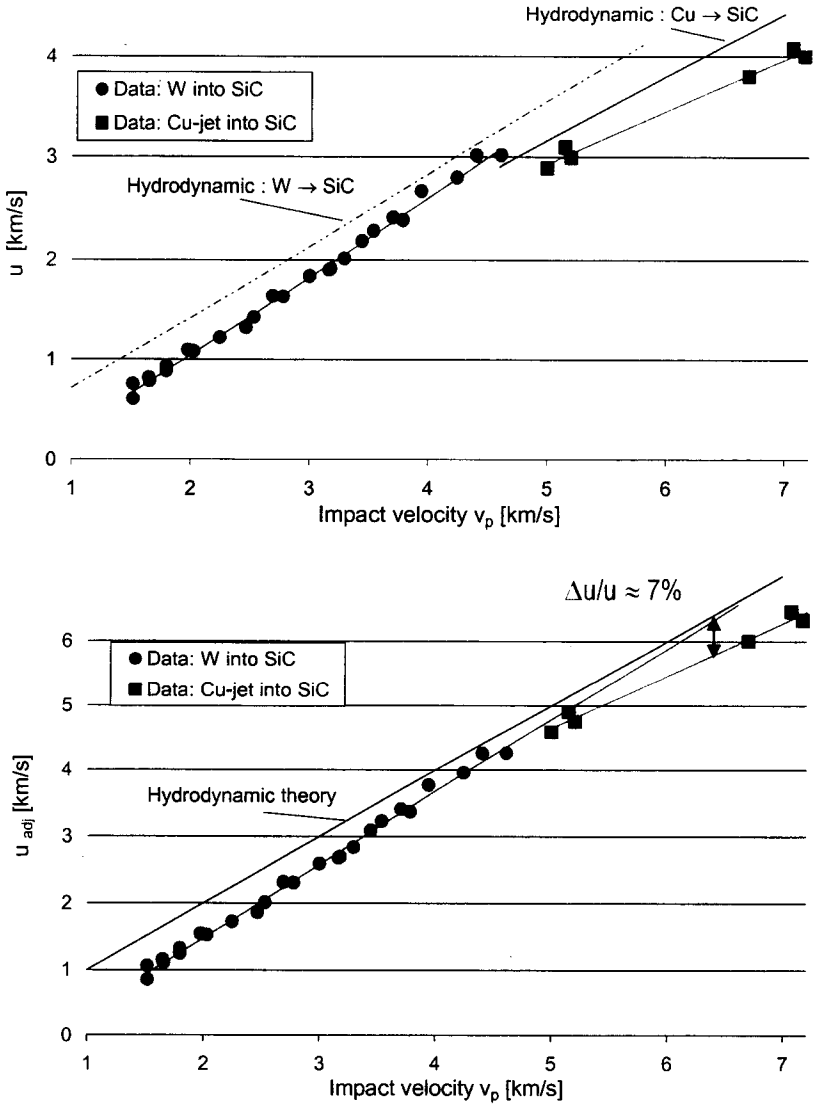

Fig: 1 Penetration-velocity in SiC for different experiments

Also shown is the hydrodynamic limit

$$u_{hyd} = v_P / (1 + (\rho_T/\rho_P)^{1/2}) \quad (1)$$

A normalized penetration velocity $u_{adj} = u(1 + (\rho_T/\rho_P)^{1/2})$ was introduced to account for the differences in projectile and target material (Fig. 1). Linear least square fits give:

for W/SiC $u_{adj} = -0.719 + 1.101\ v_P$ [km/s] (2)

and

for Cu/SiC $u_{adj} = 0.620 + 0.804\ v_P$ [km/s] (3)

The main feature of the results in [1-2] is that for the long-rod experiments the slope of

penetration velocity u is greater than, and for the shaped-charge jet experiments the slope of u is less than, the slope of the hydrodynamic limit; i.e., the penetration resistance changes at an impact velocity v_P of about 5.0 km/s ($u \approx 3.5$ km/s) and is greater in the high-velocity range. This behavior is tentatively interpreted by the existence of a failure wave. The uncertainties around that interpretation are discussed in [7] together with three additional interpretations: a) the kinetics (time dependence) of SiC failure, thus called failure kinetics, b) a possible phase transition in reaction bonded SiC and c) the differences in the two independent sets of tests. These interpretations are discussed in more detail in Ref. [7].

To eliminate the uncertainties in the analysis of the two disparate data sets, and to verify the change in slope of the penetration velocity at $u \approx 3.5$ km/s, it was decided to conduct a test series using a common set of projectile and target materials. The impact velocities for these experiments need to be varied from ~4.5 km/s to ~6.5 km/s to encompass the range of impact velocities where the slope in penetration velocity changed in [1-2]. Further, such a test series requires high measurement accuracy since the change in slope results in a reduction of the penetration velocity of only 0.3 km/s at an impact velocity of 6.5 km/s ($u \approx 4.1$ km/s, $\Delta u/u \approx$ 7%). Therefore a new set of reverse ballistic experiments has been performed specifically to eliminate the deficiencies identified in [1-2] and to improve the precision in measurement techniques compared to the standards in [1-3].

The ceramics studied are SiC-B and SiC-N from CERCOM Inc. The penetrator material was changed from pure tungsten to pure gold to eliminate strength effects of the penetrator. Tests at impact velocities between 3.5 and 4.5 km/s were performed to reproduce the essential results of the earlier work.

EXPERIMENTAL DESIGN

The targets are SiC cylinders, Type B and N (pressure assisted densification, CERCOM Inc.) with diameters of 15 mm and 20 mm, and lengths from 35 mm to 48 mm. These SiC cylinders are not confined except for a surrounding plastic sabot. The sabot is made of polycarbonate with an 8-mm Al disk behind the SiC cylinder (Fig 2). To reduce the yaw angle, the sabot does not separate from the SiC sample during free flight. Also, confined SiC-B samples identical to those used in [3] were tested. These samples have a diameter of 23.6 mm and a length of 48 mm. Both SiC-B samples, unconfined and confined, were from the lot used in [3] and were supplied by D. Orphal.

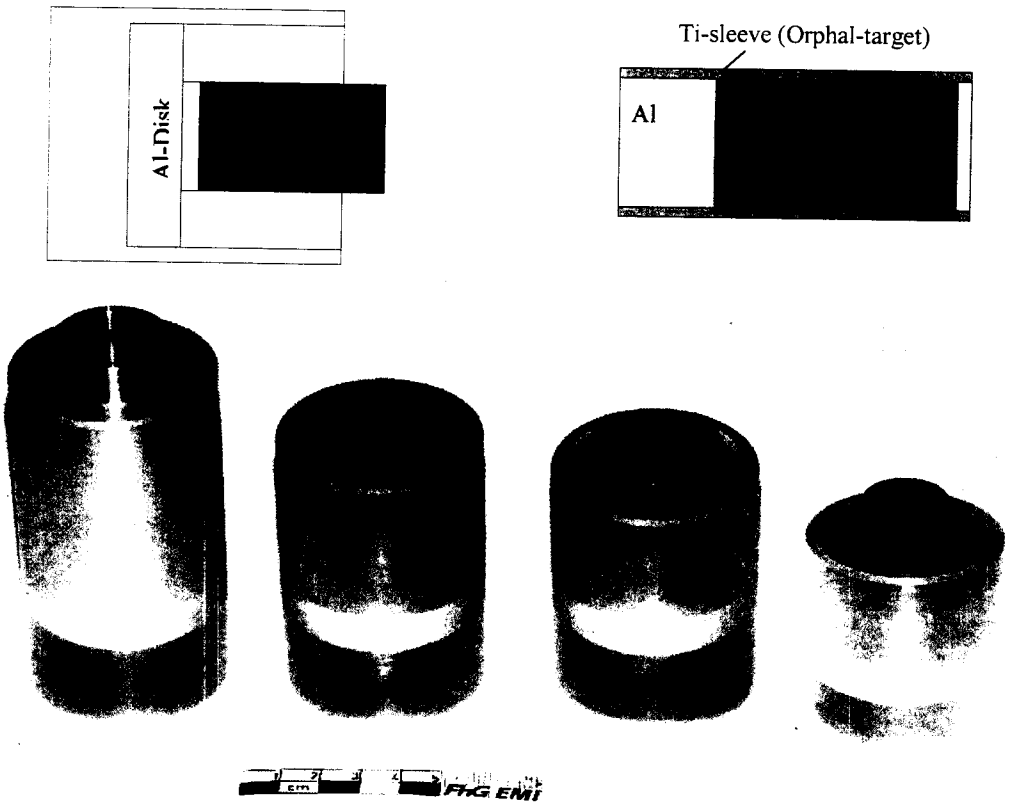

Fig. 2: SiC Targets with sabot

These variations in target parameters allow comparison of results with the older data in [3], as well as an assessment of the influence of lateral dimensions (i.e., diameter) and confinement. Some material properties of SiC are given in Table 1.

TABLE 1: Material properties for silicon carbide

Ceramic	Density [g/cm^3]	Young's mod. [GPa]	Shear mod. [GPa]	Hardness HK 0.3 [kg/mm^2]
SiC- B	3.22	427	184	2384 ± 17
SiC -N	3.21	454	195	2293 ± 42

The experiments were conducted in the reverse ballistics mode. The SiC samples were launched by a two-stage light-gas gun, pump tube caliber 150 mm, launch tube caliber 50 mm. The pump tube was filled with hydrogen at a pressure of 10 bar, the compression piston had a weight of around 13 kg. An overview of this specific gun is given in [8]

The projectiles were rods of pure (99.99%) gold (Au) instead of pure (99.95%) tungsten (W) used in [3], with a diameter of 0.75 mm and a length of 50 mm. The material properties for Au are: density 19.3 g/cm^3, hardness 65 HV 5, UTS 220 N/mm^2 and elongation 30%.

TEST SET-UP

Fig. 3 shows the experimental arrangement in- and outside the closed indoor range of the gun. Note that the sketch is not in scale. The diameter of the tank is 1.5 m.

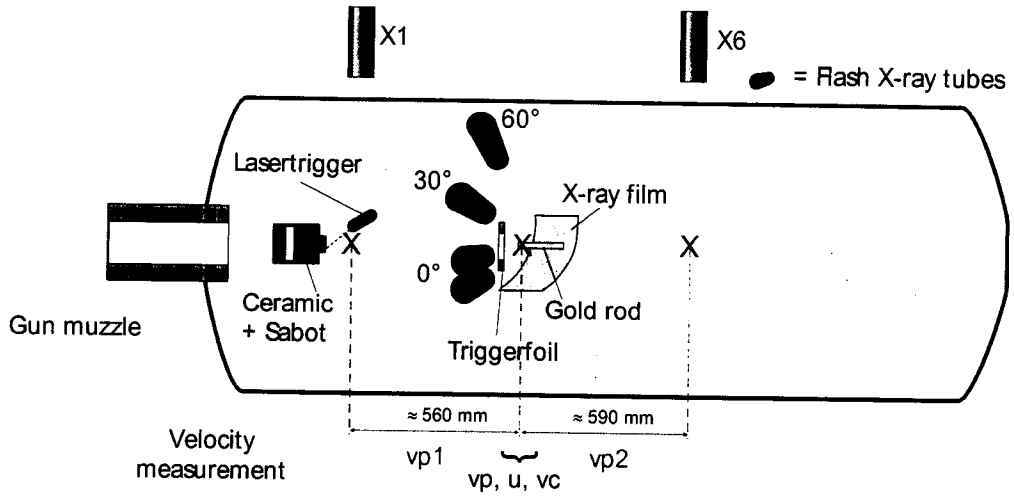

FIGURE 3: Test-set-up – reverse ballistic method

The tank was flooded with nitrogen prior to a pressure decrease to 150-200 mbar to prevent the hydrogen from reaction in the tank after launch. The Au rod was adjusted in the trajectory and aligned by laser light reflection from the blunt nose of the rod (Fig. 4) so that the yaw angle of the rod is close to 0° ($< \pm 0.1°$). The rear of the rod (the last 8 mm) is inserted in Styrofoam that is mounted on a holder, which allows an adjustment in three dimensions. The impacting target destroys the Styrofoam but not the holder, which is reused for all tests.

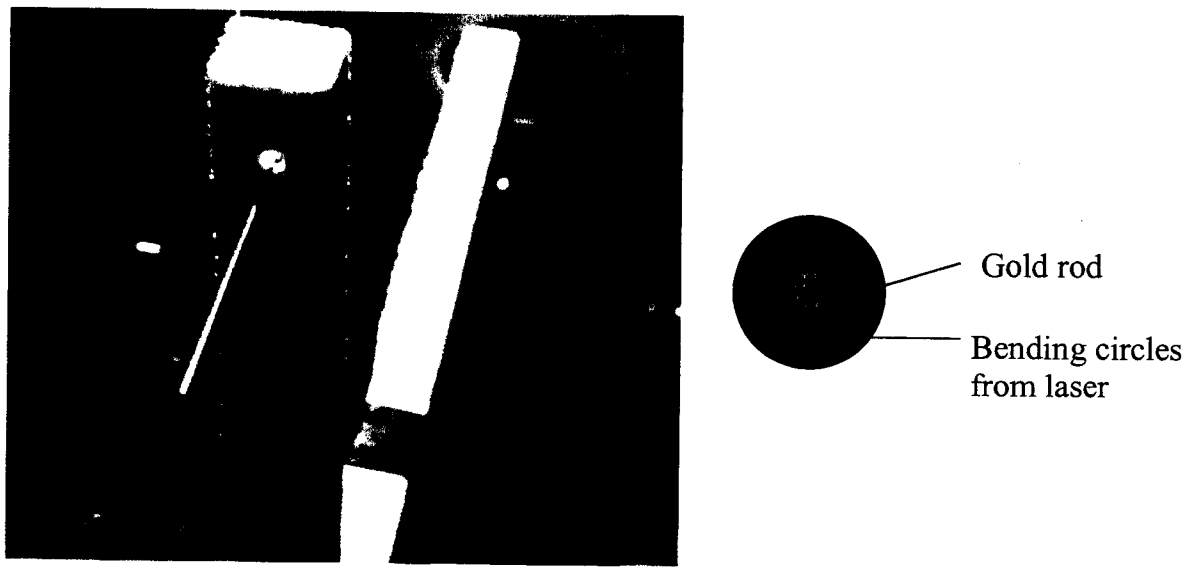

Fig 4: Rod adjustment by laser light

The rod is positioned only about 1.3 m from the gun muzzle, which keeps the yaw angle of the SiC sample as low as possible. The aim point of the gun depends on the velocity and shows a certain spread. The aim point as a function of velocity was determined by pretest experiments, and the position of the rod is adjusted accordingly.

The penetration process is observed by two 300-kV and two 450-kV flash X-ray systems, the tubes of which are aligned outside the tank in one plane normal to the line of flight. This plane is positioned at the nose end of the Au rod. The observation of the penetration process by flash radiography is completed before the SiC sample touches the Styrofoam holder of the rod; i.e. the flight distance of taking the four flash X-ray pictures is limited to about 42 mm. The longitudinal wave speed in the Au rod is around 2 km/s. Since the total time interval to observe the penetration is less than 15 μs for these experiments, the impact disturbance propagates only 30 mm into the rod. Consequently, there is no acceleration of the rod rear end during the penetration phase.

The 450-kV flash X-rays have a triple anode tube with linear alignment of the anodes. Only the two outer anodes are operated to obtain sufficient separation of the images on the film (Fig 5).

Fig. 5: 450 kV triple anode X-ray tube

The two 300-kV systems are conventional single anode tubes, which are inclined 30° and 60° with respect to the symmetry axis of the 450-kV tube. These four flash X-ray systems are operated with about 220 kV for best contrast on the developed film. The X-ray-film is inserted in a circular shaped cassette, mounted at a distance of 200 mm from, and parallel to, the line of flight (Fig. 6).

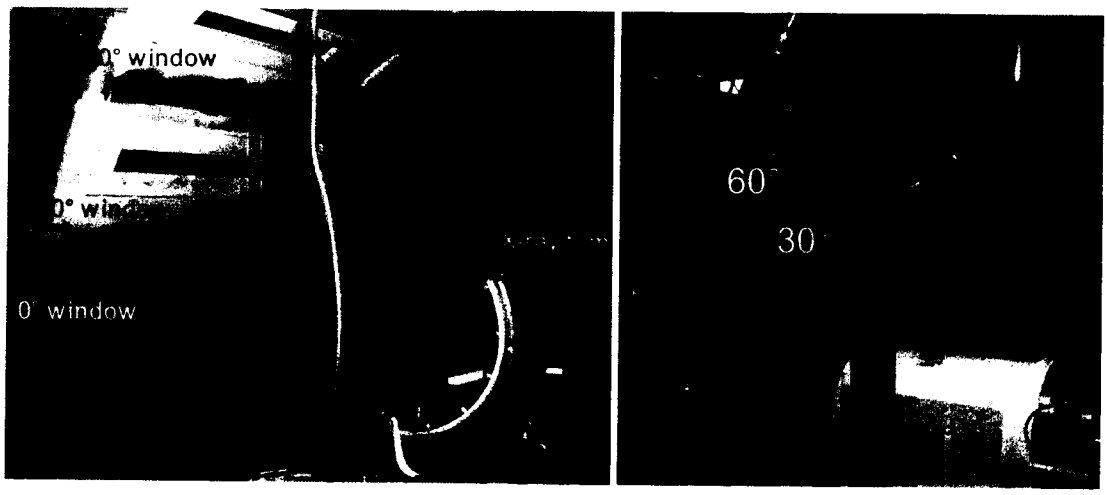

Fig. 6: Set-up inside and outside the test chamber

The four flash X-ray systems are triggered by a short circuit foil, which is fixed 15 mm in front of the Au rod. The foil has a 40-mm hole, so the plastic sabot initiates the trigger, not the SiC sample (Fig. 7). In a later series this foil was replaced by a high-intensity laser. At distances of 560 mm in front and 590 mm behind the Au rod, two additional flash X-ray pictures of the SiC sample are taken with 180-kV systems. The first one is triggered by a high intensity 300-mW laser because of the muzzle flash, the second one by the short-circuit trigger foil in front of the Au rod. Both pictures allow independent measurements of the impact velocity, which is also measured from the four flash X-rays during penetration. The times of the flash X-ray pictures and of the short circuit trigger is monitored on the same time base with two 4-channel digital oscilloscopes (resolution 0.4 ns). The current pulse in the flash X-ray systems is recorded with the oscilloscopes.

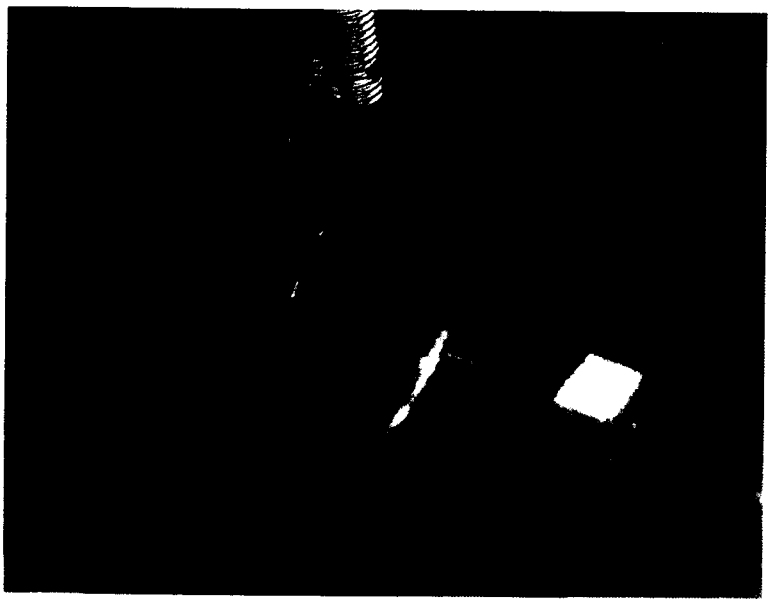

Fig. 7: Trigger method for the X-ray system

The SiC sample decelerates during free flight due to drag. Thus, $v_{P1} \geq v_P \geq v_{P2}$ is expected, where v_{P1} is the velocity at the 560-mm distance, v_P is the velocity measured in the 4 flash X-ray pictures, and v_{P2} is the velocity at the 590-mm distance. The 590 mm station was not installed in a first test series, and the velocities v_P in two of the tests were 80 and 130 m/s larger than v_{P1}. This indicated some deficiency in the accuracy of the measurements. The problem was resolved by improving the electronic auxiliary devices of the time measurement system. During the first test series, the current of the flash X-rays was measured at the tubes for the 300-kV systems and at the capacitor pot for the 450-kV system. This resulted in an additional run time through the high-voltage cable of 27 ns for the 450-kV system. Also, the pre-existing wiring had different cable types and lengths. Consequently, the facility was rewired with equal-length signal lines, and all currents were monitored at the tubes. Furthermore, the 590-mm velocity station was installed to insure velocity measurement consistency. With these changes, the measured velocities were consistent, with $v_{P1} \geq v_P \geq v_{P2}$.

ANALYSIS OF THE FLASH X-RAYS

The four flash X-ray pictures observing the penetration process were evaluated by determining the positions of the SiC sample, the stagnation point, and the rear end of the Au rod (Fig. 8). Some typical flash X-ray sequences are shown in Fig. 9. No movement of the rear end of the rod is observed.

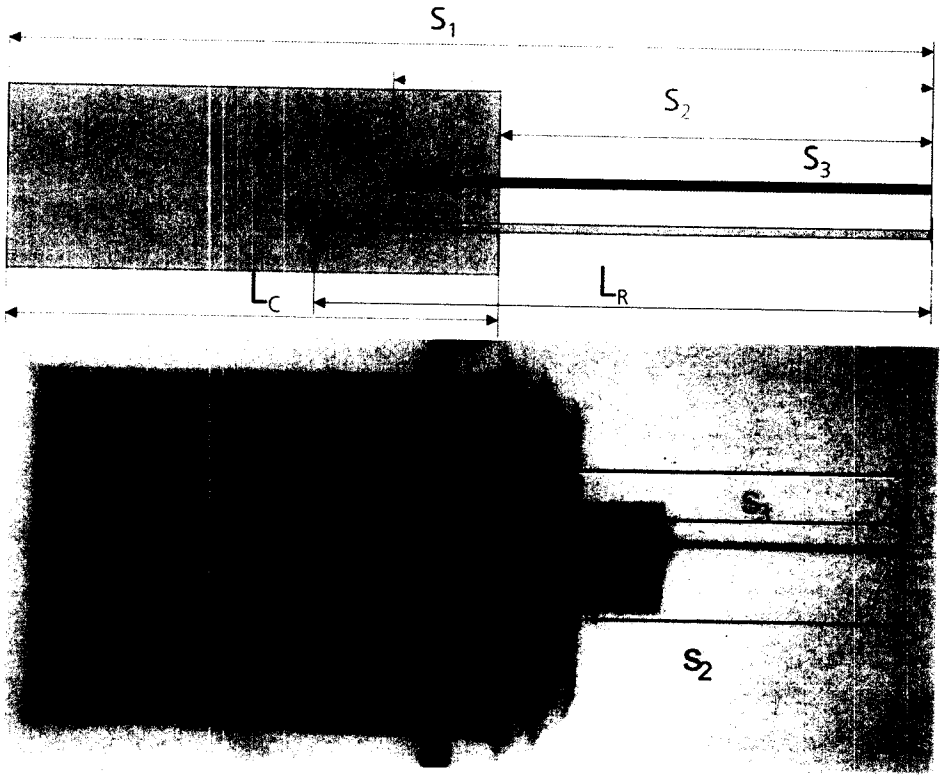

Fig. 8: Evaluation of the X-ray pictures – measured lengths

With the measured distances s_1 s_2 and s_3, as well as with the known length of the ceramic L_C and of the rod L_R, one gets the data for target travel, penetration depth and consumed length of the rod.

Target travel (v_P) = $L_R - s_3 = L_C + L_R - s_1$: proof of accuracy possible (4)

Penetration depth (u) = $s_2 - s_3$: long distances minimize error (5)

Consumed length (v_c) = $L_R - s_2$: long distances minimize error (6)

These data yield the impact velocity v_P, the penetration velocity u and the consumption velocity v_c = dl/dt. u and v_c are consistent since both velocities are determined from the position of the stagnation point. The positions are plotted versus time (of the X-ray pulses) and fit by straight lines, as shown for u and v_c for various experiments in Fig 10. The slope of the lines is the according velocity. The correlation coefficients show a strong linear relation (typically 0.999 to 1.000), so u and v_c can be considered to be constant; that is, the process is steady state [3]. The impact velocity v_P is evaluated in the same way with typical correlation coefficients of 1.000.

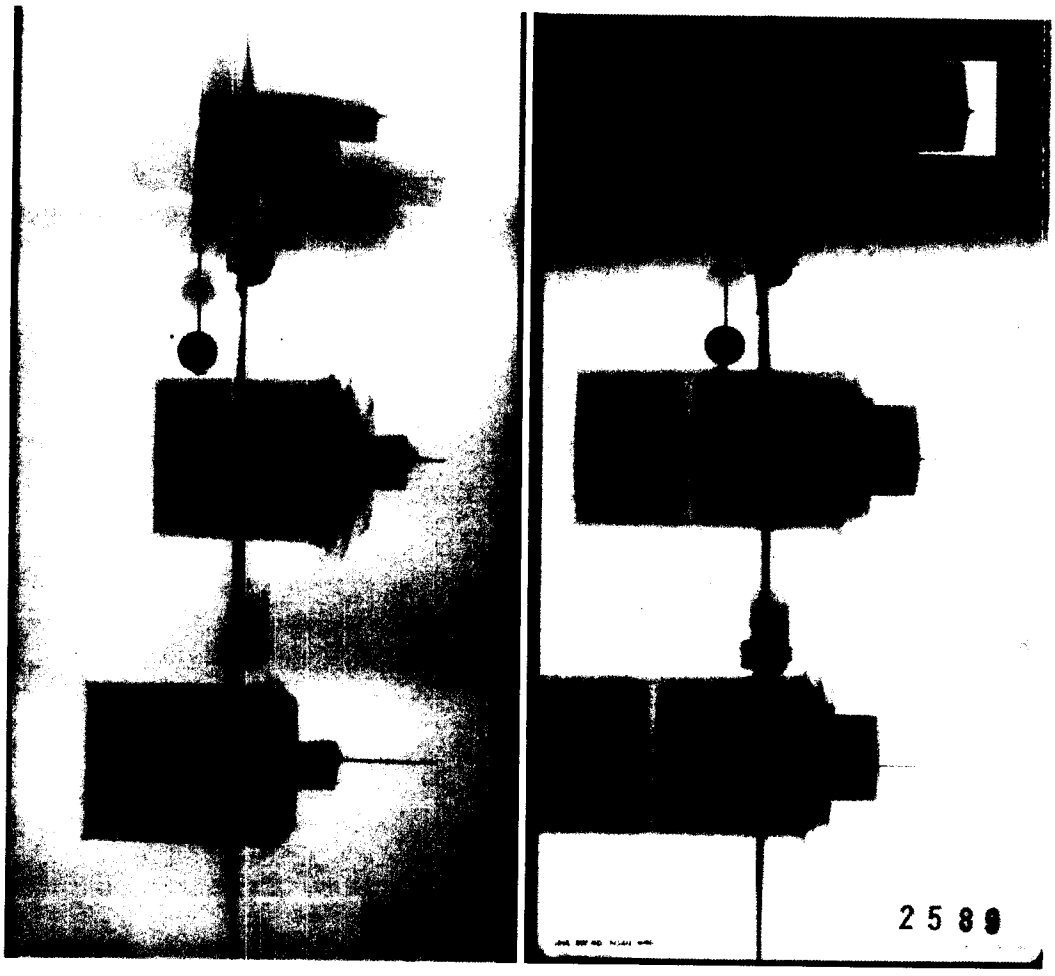

Fig. 9: flash X-ray sequence for some typical tests (right: digitally enhanced)

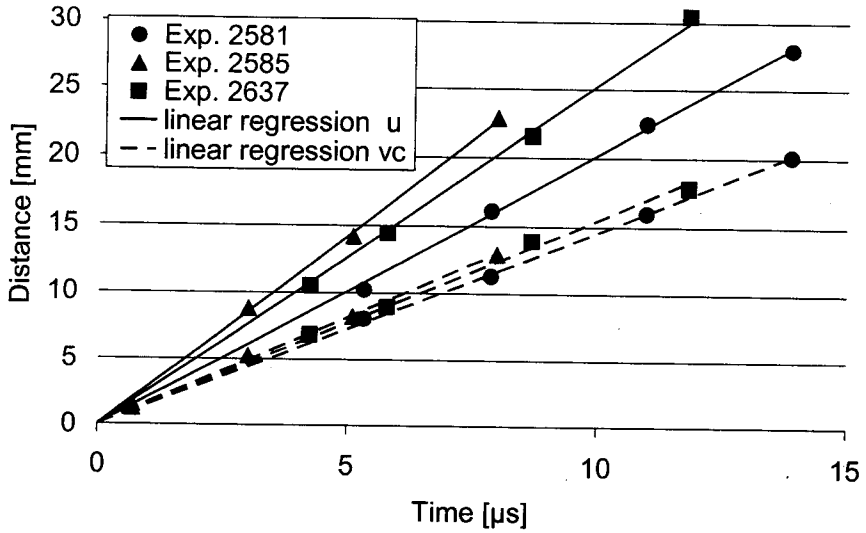

Fig. 10: Determination of u and v_P for different experiments

ACCURACY OF POSITION AND TIME MEASUREMENT

High accuracy is essential for determining the position of the SiC target with respect to the Au rod since the flight distance for taking the four flash X-ray pictures is only a few centimeters. The individual magnification factor is determined for each X-ray tube with a precision scale. A stationary picture of the SiC sample with sabot and Au rod adjusted in the actual test position is taken before every experiment. The shadowgraphs of the SiC sample and of the rod show—as does every flash X-ray shadowgraph of a solid body—a certain blur on the surface. Thus, the stationary picture together with the known dimensions of the SiC sample and the Au rod allow determining the exact position of the front or of the rear within the blur. A position accuracy of ± 0.1 mm is achieved in the actual experiment. Fiducial marks mounted in the tank at fixed positions, the shadow of which can be seen in the X-ray films, allow exact superposition of the X-ray films for evaluation. The position accuracy can be degraded somewhat by deficiencies occurring during the test, e.g., by a yaw angle, which has to be determined for every individual test. All distances are measured manually as image-processing still appears to be inferior with respect to accuracy.

Figure 11 shows a representative record of the current pulse of an X-ray station. The middle of the first pulse is taken as the time point. The accuracy is $< \pm 5$ ns.

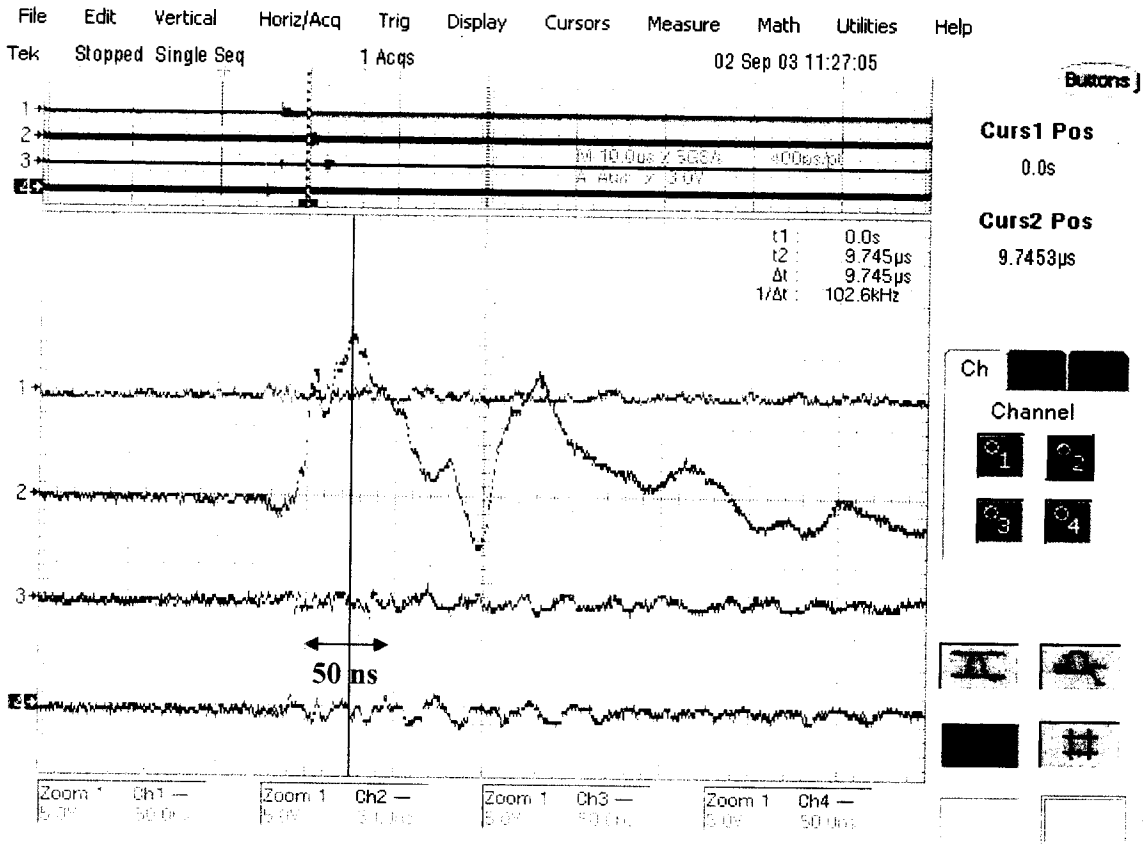

FIGURE 11: Screenshot of an X-ray signal pulse on an oscilloscope

Less accuracy is required for the long distances of 560 mm and 590 mm, the first and the last flash X-rays; thus, no stationary shadowgraph of the SiC sample with sabot was taken. The accuracy of the long distances is ± 0.2 mm. The current pulses were monitored with an oscilloscope of coarser resolution, with an accuracy of ± 0.05 µs.

The error calculation applies the accuracy of the time and distance measurement (eq. 4-6) to obtain the maximum error for the three velocities v_P, u and v_c. This is straightforward for v_P. Distance accuracy of ± 0.1 mm for the measured distances s_1 and s_3 of all 4 pictures of one experiment (eq. 4), together with the time accuracy of ± 5 ns, yields a maximum relative error of 1% for the impact velocity. The influence of the time accuracy on the resulting error is much smaller than that of the distance accuracy.

For u and v_c the error calculation is somewhat different. As u and v_c are dependent on v_P keeping v_p constant for the error calculation would mean a very small maximum error for u and v_c (only s_2 of eq. 5 + 6 would be considered). Therefore another approach was chosen to determine their maximum errors. This requires comparison against reference values for u and v_c at the maximum error impact velocity, which are the respective least-square fits for the specific ceramic tested. As there are only a few experiments for each ceramic sample—some very close together—it is not reasonable to take the actual fit for these experiments. A better procedure is to take the existing curve fit of [3] and adjust the axis intercept while maintaining

the slope. This results in a relative maximum error of roughly 1% for most of the data of u and v_c. Experiments that were difficult to analyze show a slightly larger error.

As discussed previously, the expected reduction of penetration velocity for $u \approx 4.1$ km/s is around 0.3 km/s ($\Delta u/u \approx 7\%$); therefore, the maximum error of the experiments is significantly smaller than the expected Δu of the failure kinetics effect.

EXPERIMENTAL RESULTS

The data are summarized in Table 2. In some of the tests, less than four flash X-ray pictures were taken because of experimental problems. This can reduce the measurement distance, and consequently, the accuracy of the data. Table 2 also shows the yaw angles of the impacting SiC sample and the deviation from centre impact because of the spread of the gun. Off-center impact (if the penetration comes too close to the SiC sample surface) or non-zero yaw angles can influence the data, but not the accuracy of the measurements.

TABLE 2: Test results – main parameters

Exp. No.	Target	dim. [mm]	α_1 [°]	α_2 [°]	oc x [mm]	oc y [mm]	v_{p1} [km/s]	v_p [km/s]	v_{p2} [km/s]	u [km/s]	v_c [km/s]
2581	Sic-N	15x40	0.21	-0.64	2.4	0.0	3.487	3.466 ± 1.1%	-	2.022 ± 0.5%	1.455 ± 0.7%
2567	Sic-N	15x40	0.25	0.24	-3.6	0.0	3.532	3.518 ± 1.1%	-	2.098 ± 2.0%	1.416 ± 3.5%
2584	Sic-N	15x40	-0.84	0.18	-0.9	0.0	3.610	3.688 ± 1.2%	-	2.177 ± 0.7%	1.526 ± 1.1%
2583	SiC-B	15x48	1.04	0.23	-1.9	-0.8	3.477	3.502 ± 1.3%	-	2.153 ± 1.9%	1.359 ± 1.6%
2582	SiC-B	15x48	0.46	-0.62	0.7	2.8	3.837	3.914 ± 1.3%	-	2.458 ± 1.0%	1.479 ± 0.7%
2585	SiC-B	15x48	-0.15	-0.59	-2.3	5.6	4.423	4.462 ± 1.1%	-	2.842 ± 1.7%	1.627 ± 0.9%
2589	Sic-B Ti	24x48	0.51	-0.16	-2.4	-1.6	3.373	3.504 ± 1.1%	-	2.089 ± 0.4%	1.430 ± 1.1%
2590	Sic-B Ti	24x48	0.57	-0.36	0.7	-1.2	3.489	3.587 ± 1.0%	-	2.155 ± 0.4%	1.443 ± 0.3%
2636	SiC-N	20x35	0.63	-0.16	1.6	2.0	3.646	3.618 ± 0.7%	3.554	2.214 ± 0.6%	1.426 ± 1.3%
2637	SiC-N	20x35	-0.61	0.35	2.3	4.1	4.105	4.063 ± 1.1%	4.061	2.534 ± 0.2%	1.547 ± 0.5%

v_{p1} = impact velocity ceramic measured in front of the rod (long distance measuring)
v_p = impact velocity ceramic
u = penetration velocity
v_c = consumption velocity rod
} (measured from the 4-X-rays)
v_{p2} = velocity of ceramic measured after contact with rod (long distance measuring)
oc x = off-center position of the rod for the x-axis
oc y = off-center position of the rod for the y-axis
α_1 = vertical plane angle – pitch
α_2 = horizontal plane angle – horizontal yaw

Figure 12 shows the results for u and v_c as a function of v_P for the first test series, along with two values of the improved test series, compared with the Orphal-Franzen data [3]. Generally the values are a little below the reference data for u and a little above the reference data for v_c. This can be explained by the influence of the rod material. Au has a lower strength compared to W, so the consumption velocity increases and the penetration velocity decreases. Otherwise, there is only a slight difference detectable between the SiC-N and the SiC-B targets. Even the titanium-confined SiC-B with a larger ceramic diameter shows no significant difference to the unconfined, smaller diameter samples. Off-center impact also shows no detectable influence.

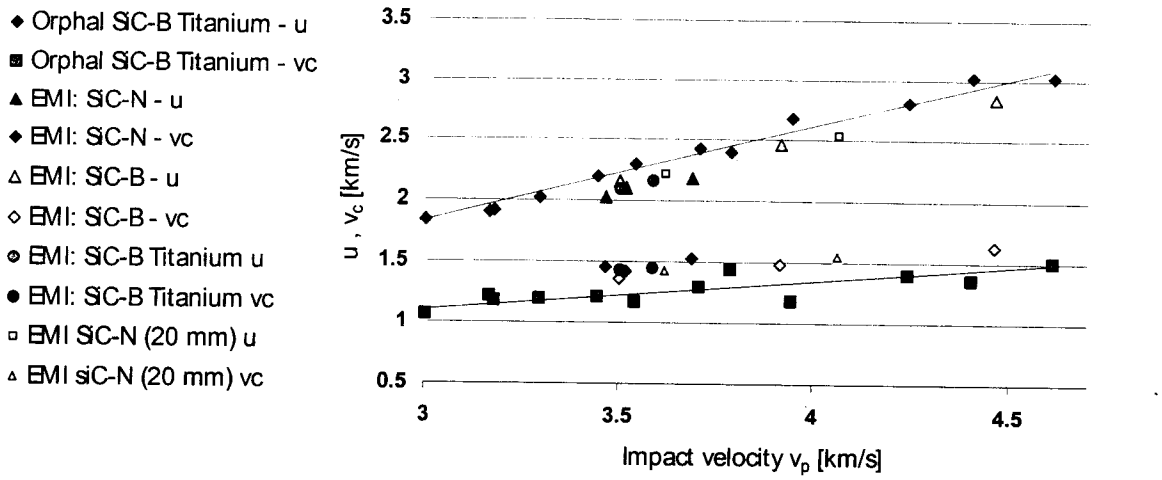

FIGURE 12: Penetration and consumption velocity as a function of impact velocity

CONCLUSIONS

The validation tests at impact velocities between 3.5 and 4.5 km/s demonstrated that a) the target redesign required to achieve higher impact velocities b) the exchange of the Orphal-Franzen SiC-B with SiC-N and c) substituting Au for W as the long-rod material have only a small effect, reducing the penetration velocity slightly. The small reduction in penetration velocity is fully in accord with the reduction in penetrator strength associated with the use of Au instead of W rods. Furthermore the error calculation showed that the sophisticated test-set-up and evaluation is able to achieve the necessary accuracy to detect the assumed failure kinetics effect. Experiments at higher impact velocities up to and above 6 km/s are currently under way and will provide useful information on the possible increase in SiC strength at high penetration velocities.

REFERENCES

1. A. A. Kozhushko, D, L. Orphal, A. B. Sinani, R. R. Franzen, "Possible detection of failure wave velocity using hypervelocity penetration experiments", *Int. J. Impact Engng.*, **23**, 467-475, 1999.
2. D. L. Orphal, A. A. Kozhushko, and A. B. Sinani, "Possible detection of failure wave velocity in SiC using hypervelocity penetration experiments", *Shock Compression of Condensed Matter, AIP*, 1999.
3. D. L. Orphal, R. R. Franzen, "Penetration of confined silicon carbide targets by tungsten long rods at impact velocities from 1.5 to 4.6 km/s", *Int. J. Impact Engng.*, **19**, 1-13, 1997.
4. G. I. Kanel, S. V. Rasorenov and V. E. Fortov, "The failure wave and spallations in homogeneous brittle materials", *Shock Compression of Condensed Matter, AIP*, 1991.
5. N. S. Brar, Z. Rosenberg and S. J. Bless, "Spall strength and failure waves in glass", *3e Congres International sur le Comportement Mechanique et Physique des Materiaux sous Sollicitations Dynamique*, 1991.
6. S. J. Bless, N. S. Brar, G. Kanel and Z. Rosenberg, "Failure waves in glass", *J, Amer. Cer. Soc.*, **75**, 1002-1004, 1992.
7. D. L. Orphal, C. E. Anderson, Jr., D. W. Templeton, Th. Behner, V. Hohler, and S. Chocron, "Using long rod penetration to detect the effect of failure kinetics in ceramics", *21st Int. Symp. on Ballistics,* Adelaide, Australia, April 2004.
8. M. Junginger: "Performance tests of a new two stage light gas gun at the Ernst-Mach-Institut" Aeroballistic Range Association, Sendai, Japan, 21.25.10.2002